Journal of Chemical&Engineering Data

pubs.acs.org/jced Article

Density, Viscosity, and Surface Tension of Aqueous 1-Methylpiperazine and Its Carbonated Solvents for the CO_2 Capture Process

Vaibhav Vamja, Chetna Shukla, Rajib Bandyopadhyay,* and Sukanta Kumar Dash*

Cite This: *J. Chem. Eng. Data* 2024, 69, 904−914 Read Online

ACCESS | Metrics & More | Article Recommendations | Supporting Information

ABSTRACT: Physicochemical properties of amine solutions like density, viscosity, and surface tension results are indispensable for designing carbon dioxide (CO_2) absorption and regeneration columns, and they are also crucial for modeling and simulation for CO_2 capture applications using the postcombustion capture method. In the present work, the density and viscosity of 1-methylpiperazine (1-MPZ) solution are studied for the temperature range of 298.15 to 348.15 K. Surface tension measurements for temperatures ranging from 303.15 to 348.15 K are reported for various concentrations of 1-MPZ. To validate the instrumental accuracy and procedure, properties of aqueous 0.3 weight fraction (w) monoethanolamine (MEA) were first measured and compared with reported results before the study of 1-MPZ. The weight fraction of 1-MPZ was kept at 0.1, 0.2, 0.3, and 0.4 for the physical property study of unloaded aqueous 1-MPZ, and 0.3w was considered for CO_2-loaded properties. The 1-MPZ solution was loaded with CO_2 up to 0.45 mol CO_2/mol amine. The Redlich−Kister equation for excess molar volume was used to correlate the measured density of the fresh and CO_2-loaded solvents. The viscosity data of unloaded aqueous 1-MPZ and CO_2-loaded aqueous 1-MPZ were correlated using the Grunberg−Nissan and modified Weiland models, respectively. Surface tension results of fresh and CO_2-loaded 1-MPZ were fitted by a polynomial function. These new data and models are helpful for the design of postcombustion CO_2 capture using 1-MPZ-based solvents and their blends.

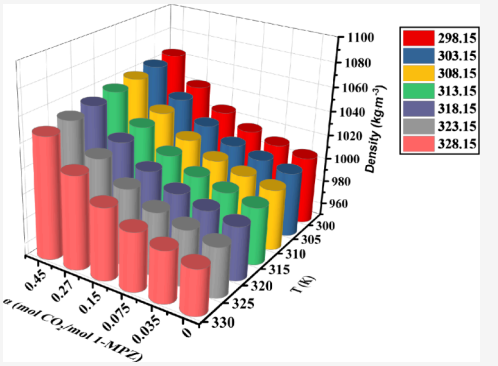

1. INTRODUCTION

Capturing CO_2 from industrial exhaust using different amine solutions with postcombustion capture technology (PCC) is a proven method, and its deployment is necessary to address industrial decarburization.[1] Aqueous solutions of amines, alkanolamines, ionic liquids (ILs), and recently some amino acids have also been used as absorbents for CO_2 removal.[2] However, an energy-efficient solvent is essential for the PCC of CO_2 in a regenerative chemical absorption process. This technology requires more research on the selection of solvent as all of the currently used solvents, like monoethanolamine (MEA), diethanolamine (DEA), di-2-propanolamine (DIPA), etc., have certain drawbacks. MEA is widely used as a reference solvent as it has a high rate of reaction as well as a lower cost.[3,4] Due to some drawbacks like thermal degradation and oxidative degradation, corrosion, and higher regeneration energy requirement, it is not accepted widely.[5−7]

Recent studies show that piperazine (PZ) and its derivatives 1-methyl-piperazine (1-MPZ) and 1-ethyl-piperazine (1-EPZ) have higher reaction rates for CO_2 capture when compared to MEA.[8−10] Both PZ and 1-MPZ exhibit resistance to thermal and oxidative degradation. Still, due to the lower solubility of PZ in aqueous solutions, 1-MPZ is preferred for concentrated solvents.[11−13] Concentrated solvents exhibit a higher cyclic capacity for CO_2 uptake.[14] 1-MPZ has a cyclic structure, as shown in Figure 1. It consists of one secondary amine group and one hindered (tertiary) amine group, and its pK_a value is highly favorable for CO_2 reaction. 1-MPZ can also be used as an efficient reaction rate promotor by blending it with a tertiary amine such as methyldiethanolamine (MDEA) or a sterically hindered amine such as 2-amino-2-methyl-1-propanol (AMP), as they have a low rate of reaction.[15,16] Among the PZ

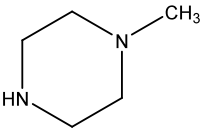

1-methylpiperazine

Figure 1. Schematic representation of 1-MPZ.

Received: November 2, 2023
Revised: January 31, 2024
Accepted: February 1, 2024
Published: February 13, 2024

https://doi.org/10.1021/acs.jced.3c00651
J. Chem. Eng. Data 2024, 69, 904−914

derivatives, 1-MPZ is liquid at room temperature, and its heat absorption is comparatively less with greater cyclic capacity.[17,18] So, 1-MPZ has been chosen as a potential candidate for the CO_2 capture solvent selected in this work.

A study of physicochemical properties and data is required for the design of the CO_2 capture process.[19,20] Properties like density, viscosity, and surface tension at a wide range of temperatures and compositions are essential to understanding the physical solubility and diffusivity of CO_2 in the aqueous solutions.[21,22] Viscosity also plays a vital role in the mass transfer of CO_2 in the solvent. Solvents having higher viscosity values are not ideally preferred due to their higher resistance in mass transfer.[3] The diffusion coefficient declines with an increase in solvent viscosity, resulting in a decrease in the absorption rate.[23] The mass transfer performance of liquid is directly related to the wetting area of the absorber column's packing material, which can be understood from surface tension results.[24]

Although 1-MPZ is proven to be a promising solvent, very little literature is available on the physicochemical properties of 1-MPZ. Rayer et al.[25] studied these properties for 0.25*w* to pure 1-MPZ solutions. Chen et al.[26,27] studied thermophysical properties and vapor−liquid equilibria for 1-MPZ using alcohols such as methanol, *n*-propanol, and *n*-butanol as solvents. Yang et al.[28] studied the volumetric properties and viscosity of 1-MPZ using methylcyclohexane and *n*-heptane as solvents. Although limited literature on the thermophysical properties of 1-MPZ-based aqueous and nonaqueous solvents is available, the physicochemical properties of CO_2-loaded aqueous 1-MPZ systems are unavailable despite their importance in process design and simulation. Hence, in this work, properties such as density, viscosity, surface tension, and molar volume of unloaded aqueous 1-MPZ and CO_2-loaded aqueous 1-MPZ solutions have been studied at various temperatures and compositions and reported. The concentration of aqueous 1-MPZ has been chosen in the range of 0.1 to 0.4*w* fractions as usually, in industrial practices, a 0.3*w* amine concentration or less is used for the CO_2 removal process.[29] More than 0.4*w* concentration is not generally used, as it leads to problems such as viscosity, corrosivity, degradation, and environmental and safety concerns. In addition, 1-MPZ is used with some other amines in a blended solvent, and its concentration is kept below 0.3*w*.[14] Hence, the range of 0.1 to 0.4*w* 1-MPZ concentrations has been chosen in this study.

2. EXPERIMENTAL SECTION

2.1. Materials. Chemical details and sample purity are presented in Table 1. Deionized water (double distilled) was used to prepare all of the solutions by weight measured using a Mettler Toledo weighing balance model ME 204. The accuracy of this balance was ±0.0001 g.

Table 1. Chemical Sample Details

chemical	abbreviation	CAS number	purity (mass fraction)	supplier
1-methylpiperazine	1-MPZ	109-01-3	=0.99	Sigma-Aldrich
monoethanolamine	MEA	141-43-5	≥0.99	Sigma-Aldrich
carbon dioxide	CO_2	124-38-9	≥0.99	Linde India Ltd.

2.2. Density Measurement. A density meter, Anton Paar DMA 4500, was used to measure the density of the solutions. The repeatability of the density meter for temperature was ±0.001 °C, and for density, repeatability was ±0.01 kg/m^3. The instrument contained one U tube and a PT100 platinum resistance thermometer. The density of the solution is proportional to the oscillation frequency, and it can be expressed by eq 1.

$$\rho/\mathrm{g\cdot cm^{-3}} = A + B\tau^2 \tag{1}$$

Here, ρ is the density of the solution, and τ (s) is the period of oscillation. The density meter was calibrated with air and water at 293.15 K. The density was measured at atmospheric pressure. Density measurements for demineralized (DM) water were performed from 298.15 to 348.15 K. The obtained results were compared with the literature data. The density of 0.3*w* MEA was measured from 298.15 to 348.15 K. The results were compared with those of Hartono et al.[30] and are listed in Table S2 of the Supporting Information. The average absolute deviation (AAD) between measured and reported values was obtained following eq 2. AAD% between experimental and reported values was found to be below 0.1%. The expanded uncertainty for the density measurements, $U_c(\rho)$, was 0.559 kg/m^3 for unloaded 1-MPZ solutions. Similarly, for the CO_2-loaded 1-MPZ solution, the expanded uncertainty was found to be 1.521 kg/m^3 (level of confidence = 0.95).

$$\mathrm{AAD}(\%) = [(100/N)\cdot \sum_i^N ((\rho_{\mathrm{experimental}} - \rho_{\mathrm{reported}}) / \rho_{\mathrm{experimental}})] \tag{2}$$

2.3. Viscosity Measurement. The viscosity of 1-MPZ was investigated using a Cannon Fenske viscometer. The viscometer was calibrated using water. First, the viscosity of the DM water was measured. After that, viscosity measurement for unloaded aqueous 1-MPZ was carried out using the same viscometer. The intended temperature range of 298.15 to 348.15 K was used to measure the viscosity. From published data, the water viscosity was verified. After that, a viscometer was used to measure the solution's viscosity. The viscometer was cleaned with methanol after completing the experiment. The following equations were used to calculate the dynamic viscosity from flow time.

$$\vartheta = \text{viscometer constant} \times t_w \tag{3}$$

From eq 3, we get the kinematic viscosity of water in the centistokes (cst) unit. From the kinematic viscosity and density of water for the corresponding temperature, dynamic viscosity was calculated using eq 4.

$$\mu_w = \vartheta \times \rho_w \tag{4}$$

Here, μ_w represents dynamic viscosity in cP (centipoise). ρ_w is the density of water.

By putting all of the values in eq 5, the dynamic viscosity of 1-MPZ was obtained.

$$\mu_s = \frac{\rho_s \times t_s \times \mu_w}{\rho_w \times t_w} \tag{5}$$

Here, μ_s is the kinematic viscosity of the 1-MPZ solution, ρ_s is the density of the solution, and t_s is the flow time for the solvent. Before measuring the viscosity of 1-MPZ, viscosity

https://doi.org/10.1021/acs.jced.3c00651
J. Chem. Eng. Data 2024, 69, 904−914

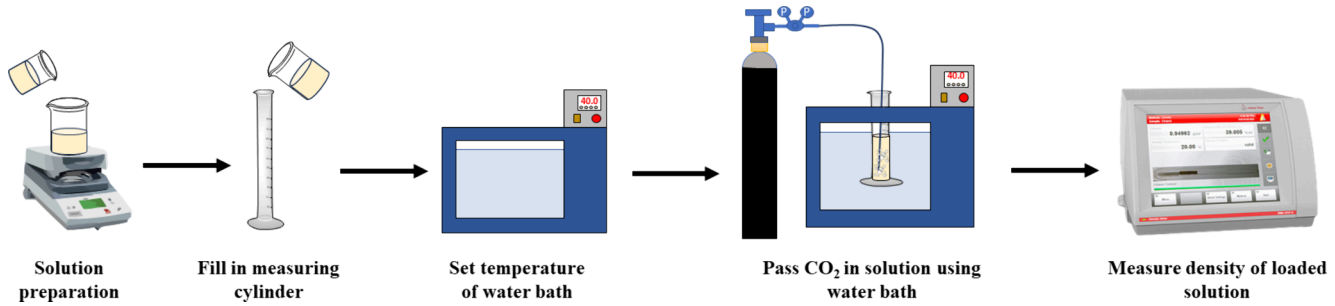

Figure 2. CO_2 bubbling process diagram.

Table 2. Density of Unloaded Aqueous and Pure 1-MPZ Solutions at Atmospheric Pressure[a]

	density ρ (kg·m^{-3})				
T/K	w(1-MPZ) = 0.1	w(1-MPZ) = 0.2	w(1-MPZ) = 0.3	w(1-MPZ) = 0.4	w(1-MPZ) = 1.0
298.15	997.73	1003.03	1005.65	1010.12	898.91
303.15	996.12	1000.53	1002.71	1006.42	894.57
308.15	994.28	997.85	999.68	1002.60	890.17
313.15	992.26	995.03	996.59	998.73	885.74
318.15	990.06	992.09	993.35	994.79	881.30
323.15	987.69	989.03	989.99	990.80	876.84
328.15	985.16	985.82	986.51	986.74	872.35
333.15	982.48	982.54	982.96	982.61	867.84
338.15	979.65	979.12	979.29	978.42	863.31
343.15	976.69	975.59	975.53	974.16	858.76
348.15	973.59	971.96	971.62	969.83	854.20

[a]The uncertainties are given in Table 15.

data of 0.3w MEA were generated using the same procedure and compared with the results reported by Amundsen et al.[31] and Hartono et al.[30] to validate the instrument's accuracy and procedure. These validation results are listed in Table S3 of the Supporting Information. AAD% was calculated according to the literature, and obtained results were found to be ≅0.2%. The expanded uncertainty of viscosity results of the unloaded 1-MPZ solution was 0.410 mPa·s, and for the CO_2-loaded 1-MPZ solution, it was 0.869 mPa·s (level of confidence = 0.95).

2.4. Surface Tension Measurement. Surface tension is an important parameter for checking the PCC process's solvent compatibility. The surface tension of solutions was measured using a Kyowa DY-300 surface tensiometer. The accuracy of the Kyowa DY-300 surface tensiometer was 0.2 mN/m. The surface tension of 0.3w MEA was measured for the temperature range T = 303.15 to 348.15 K with 5 K intervals. Using the Wilhelmy plate method, Vázquez et al.[32] performed experiments to measure the surface tension of MEA and other solvents. Results are listed in Table S4 and compared with the literature data. AAD% was calculated and found to be ≅0.1%, which agrees with the reported data. The expanded uncertainty of surface tension $U_c(\gamma)$ measurement for the unloaded 1-MPZ solution was 0.731 mN/m, and for the CO_2-loaded 1-MPZ solution, it was 1.673 mN/m (level of confidence = 0.95).

2.5. Measurement of CO_2-Loaded Properties. The density, viscosity, and surface tension of the CO_2-loaded 0.3w 1-MPZ solvent were determined using the same instruments used for the fresh solvents. CO_2 loading was performed by bubbling CO_2 gas into a freshly prepared 0.3w 1-MPZ solvent. For that, the solution was filled in a 100 mL measuring cylinder. Then, this cylinder containing the solution was put into a water bath, which was set at a specific temperature. The CO_2 loading process was performed under atmospheric pressure. After the required temperature of the solution was achieved, CO_2 was passed from the CO_2 cylinder for a specific period of time. The valve was used to control and maintain a constant flow of gas in solution. Aluminum foil was used to cover the cap of the measuring cylinder to restrict evaporation loss, if any. In addition, it was ensured that the initial and final volume should be the same. Any minute, an evaporation loss (if any in any observation) was made with water, assuming that water would have evaporated, causing a volume change. Again, no precipitation formation was found during the CO_2 loading experiments within the experimental conditions reported in this work. Figure 2 illustrates the CO_2 loading process. A similar approach was applied by Freeman et al.[33] for CO_2 loading. The loading was determined by the density difference method. The density of this prepared solution was measured before the loading of CO_2 gas. The density of the CO_2-loaded solvent was measured with the same density meter. During density measurement, the volume of the solution remains the same. So, an increase in density was considered as the weight of CO_2 in the loaded solution. From the weight of CO_2 absorbed in the solution, moles of CO_2 in the solution was calculated. The CO_2 loading can also be determined using the acid−base titration method.[34,35] To validate the results of the density difference method for obtaining the CO_2 loading, acid−base titrations were conducted.[34,35] Both of the results are compared and presented in Table S1 and Figure S1 of the Supporting Information. The AAD% between the two methods was found to be 3.14. This difference was considered in the uncertainty calculation of the properties of the CO_2-loaded solution.

We have used 0.3w 1-MPZ from all these concentrations to study loaded properties because 0.3w MEA is considered a

https://doi.org/10.1021/acs.jced.3c00651
J. Chem. Eng. Data 2024, 69, 904−914

benchmark solution for CO_2 capture.[36] The 0.3w MEA solution is used in the industry-scale implementation of CO_2 capture.[37] Also, for studying blends, the total concentration is kept at 0.3w so that results can be easily compared with the available literature.[38,29] To maintain this uniformity, we kept a 0.3w concentration for the CO_2 loading study.

3. RESULTS AND DISCUSSION

Experimental results of density, viscosity, and surface tension measurements and modeling of the binary mix 1-MPZ-H_2O and the ternary mix 1-MPZ-H_2O-CO_2 are presented in subsequent sections.

3.1. Density. Densities of aqueous 1-MPZ solutions have been studied for temperatures ranging from 298.15 to 348.15 K. Weight fractions of the solvent studied were 0.1w, 0.2w, 0.3w, 0.4w, and pure 1-MPZ. The obtained density values of 0.1w, 0.2w, 0.3w, 0.4w, and pure 1-MPZ solutions are listed in Table 2. All the reported values of densities are the average of two measurements. Before each run, the density meter is calibrated with the density measurement of air and deionized water. From the results of Table 2, it is noticed that the density values of 1-MPZ tend to increase with an increase in concentration and decrease with an increase in temperature. The density of pure 1-MPZ is the lowest among all of the aqueous solutions. The results show that with an increasing concentration of 1-MPZ, the density increases, although the density of pure 1-MPZ is the lowest. This behavior of the 1-MPZ mixture is due to the nonideal nature of the solution. When two nonideal behaving components are mixed to form the solution, it either expands or shrinks. When pure 1-MPZ is added to the water, the solution volume decreases slightly. As the density is inversely proportional to the volume of the solution, it results in an increase in the density of the solution. This shrinkage in the volume is also confirmed from the negative excess molar volume results presented in Table 4 and Figure S2 in the Supporting Information. From Figure 3, a crossover of results is observed between aqueous 1-MPZ density at a temperature of 333.15 K. For a lower 1-MPZ concentration, the solution shows a smaller decrease in density with an increase in temperature. This trend is similar to that of water. For higher concentrations of 1-MPZ density, values show a greater decrease in density with increasing temperature, similar to pure 1-MPZ. The values of pure 1-MPZ are compared with the results in the literature and presented in the Supporting Information in Table S5. AAD% between experimental and literature results is 0.013%.

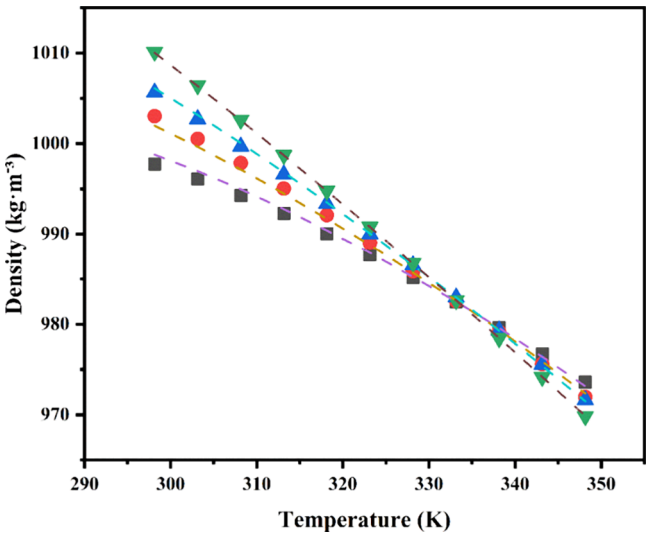

Figure 3. Density of unloaded aqueous 1-MPZ solutions at various temperatures and concentrations (mass fraction): green triangles, 0.4; blue triangles, 0.3; circles, 0.2; squares, 0.1. Dashed lines in the graph represent Redlich−Kister correlation between density and temperature.

The density of the CO_2-loaded 0.3w aqueous 1-MPZ solvent was measured at T = 298.15−328.15 K. CO_2 is loaded up to 0.45 mol CO_2/mol 1-MPZ. CO_2 loading is performed with precision at atmospheric pressure. Results are listed in Table 3. The density increases with an increase in the CO_2 loading. With a rise in temperature, the trend remains the same. The density decreases with increasing temperature.

The experimental density results reported in this work have been further correlated using the Redlich−Kister equation presented in eq 6. This equation is applied to determine the excess molar volume for the binary or ternary system. The equation is a function of molar composition and temperature and is provided by the following equation:

$$V_{jk}^{E}(\mathrm{m^3{\cdot}kmol^{-1}}) = x_j{\cdot}x_k \sum_{p=0}^{n} A_p(x_j - x_k)^p \tag{6}$$

where x_j and x_k are the mole fractions of the components, A_p is the adjusted parameters, and n represents the number of adjusted parameters. Here, A_p is again correlated using a quadratic equation, which is temperature-dependent and is given by eq 7.

$$A_p = l + m{\cdot}T + n{\cdot}T^2 \tag{7}$$

Authors have also adopted this approach to represent the excess molar volume of the binary or ternary system.[39−41]

The experimental density calculates the amine solution's excess molar volume, expressed by eq 8.

$$V^E = V_m - \sum x_i V_i^0 \tag{8}$$

where V_i^0 is the volume of the pure component in the aqueous amine mixture and V_m represents the molar volume of the amine mixture at a specified temperature calculated using eq 9.

$$V_m = \frac{\sum x_i M_i}{\rho_m} \tag{9}$$

where ρ_m is the experimentally measured density. x_i and M_i represent the mole fraction and molar mass, respectively.

The excess molar volume of 1-MPZ is calculated from the measured density values using eq 8. Variation in the excess molar volume is measured with changes in the concentration of components and temperature. Table 4 contains excess molar volume results for the corresponding density values. From the results obtained, it is evident that the excess molar volume decreases with an increasing concentration of 1-MPZ. The negative results confirm strong interactions between water and 1-MPZ molecules.[42,43] The decrease in the volume can be explained by the tendency of 1-MPZ molecules to occupy the voids between water molecules.[44] Also, the formation of hydrogen bonds between 1-MPZ and water molecules can be considered one of the possible reasons for the volume contraction of 1-MPZ solutions.[44,45] As the temperature increases, there is a slight drop in the excess molar volume

https://doi.org/10.1021/acs.jced.3c00651
J. Chem. Eng. Data 2024, 69, 904−914

Table 3. Density of CO_2-Loaded Aqueous 1-MPZ Solutions at Atmospheric Pressure[a]

	loading α (mol CO_2/mol 1-MPZ)					
T/K	0	0.035	0.075	0.15	0.27	0.45
298.15	1005.7	1010.1	1015.6	1025.9	1042.0	1064.1
303.15	1002.7	1007.4	1012.8	1023.2	1039.4	1061.7
308.15	999.67	1004.1	1009.9	1020.4	1036.7	1059.1
313.15	996.59	1001.2	1006.8	1017.3	1033.9	1056.4
318.15	993.35	997.97	1003.7	1014.3	1030.9	1053.6
323.15	989.99	994.88	1000.4	1011.1	1027.9	1050.8
328.15	986.51	991.52	997.06	1007.8	1024.8	1047.8

[a]The uncertainties are given in Table 15. w(1-methylpiperazine) = 0.3.

Table 4. Excess Molar Volume from the Density of Unloaded Aqueous 1-MPZ Solutions at Atmospheric Pressure

	excess molar volume V^E ($m^3 \cdot mol^{-1}$) 10^{-6}			
T/K	w(1-MPZ) = 0.1	w(1-MPZ) = 0.2	w(1-MPZ) = 0.3	w(1-MPZ) = 0.4
298.15	−0.229	−0.602	−0.990	−1.523
303.15	−0.232	−0.595	−0.983	−1.506
308.15	−0.236	−0.590	−0.978	−1.490
313.15	−0.239	−0.584	−0.975	−1.476
318.15	−0.243	−0.580	−0.972	−1.464
323.15	−0.247	−0.577	−0.969	−1.454
328.15	−0.251	−0.574	−0.968	−1.445
333.15	−0.254	−0.571	−0.966	−1.436
338.15	−0.257	−0.568	−0.965	−1.429
343.15	−0.264	−0.569	−0.967	−1.426
348.15	−0.270	−0.570	−0.969	−1.422

of the solution, which can be due to the decrease in intermolecular H-bonding between 1-MPZ and water.

From the calculated values of V^E, density results are regressed using eq 6. A total of 55 data points were used to correlate parameters. The temperature-dependent parameters are presented in Table 5.

Table 5. Parameters of the Redlich−Kister Equation in Equations 6 and 7, for the V^E of 1-MPZ (1) + H_2O (2)

parameters		1-MPZ + H_2O
A_0	l	−0.471758792
	m	0.003162859
	n	-5.22×10^{-6}
A_1	l	−0.920470057
	m	0.006735075
	n	-1.15×10^{-5}
A_2	l	−0.494765213
	m	0.003804202
	n	-6.66×10^{-6}

Here, A_0, A_1, and A_2 are Redlich−Kister parameters, and l, m, and n represent Redlich−Kister temperature coefficients. The experimental and model-predicted density results are presented in Figure 3. It is evident from Figure 3 that the results of the observed and Redlich−Kister correlation predicted are in good agreement.

For the measured density in the CO_2-loaded solution, eq 6 is considered for the ternary system (1-MPZ + H_2O + CO_2). The Redlich−Kister equation for a three-component system is derived using the expression shown in eq 10.

$$V^E = V_{12}^E + V_{13}^E + V_{23}^E \quad (10)$$

The parameters for the loaded density data are presented in Table 6. To correlate the parameters for the CO_2-loaded

Table 6. Parameters of the Redlich−Kister Equation in Equations 6 and 7, for V^E of 1-MPZ (1) + H_2O (2) + CO_2 (3)

parameters		1-MPZ + H_2O	1-MPZ + CO_2	H_2O + CO_2
A_0	l	−0.01921	−0.06378	−0.00488
	m	8.64×10^{-5}	0.00037	2.83×10^{-5}
	n	-1.33×10^{-7}	-8.39×10^{-7}	-6.50×10^{-8}
A_1	l	−0.01921	−0.06377	−0.00498
	m	−0.00010	−0.02965	1.88×10^{-5}
	n	1.58×10^{-7}	5.14×10^{-6}	-6.49×10^{-8}
A_2	l	−0.01921	−0.06392	−0.00488
	m	0.00012	0.28521	9.13×10^{-6}
	n	-1.88×10^{-7}	−0.00015	-6.62×10^{-8}

density in eq 6, 42 data points have been used. The regression of eq 6 for binary and ternary systems was performed in MATLAB for different concentrations and temperatures. The obtained AAD% values for the fresh and the CO_2-loaded solutions are 0.02 and 0.23, respectively. The experimental and correlated density data for carbonated solutions are presented in Figure 4, which indicate good agreement with the model and experiment results.

3.2. Viscosity. Table 7 shows the viscosity results of 1-MPZ at temperatures ranging from 298.15 to 348.15 K for 0.1w, 0.2w, 0.3w, 0.4w, and pure 1-MPZ. Two measurements were performed for each temperature, and the average value is considered as the result. This work's experimental results of pure 1-MPZ are compared with the reported data by Rayer et al.[25] This comparison is presented in Table S6. The viscosity of a solution depends on the structure of the individual molecules

https://doi.org/10.1021/acs.jced.3c00651
J. Chem. Eng. Data 2024, 69, 904−914

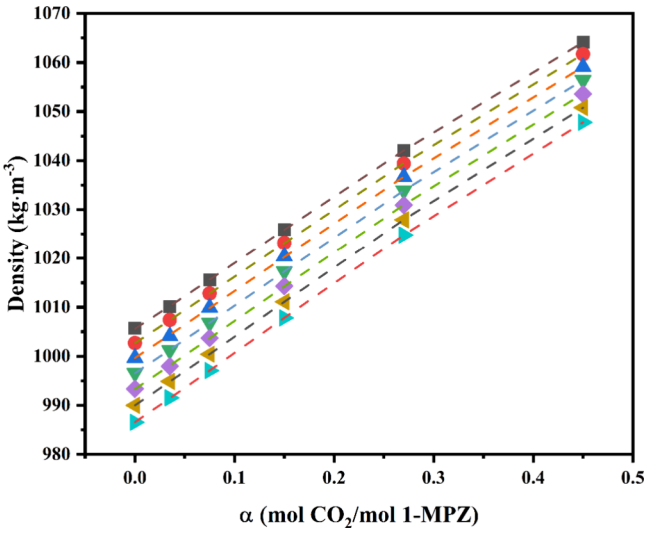

Figure 4. Density of CO_2-loaded 0.3w aqueous 1-MPZ at various temperatures: squares, 298.15 K; circles, 303.15 K; blue triangles, 308.15 K; green triangles, 313.15 K; diamonds, 318.15 K; yellow triangles, 323.15 K; cyan triangles, 328.15 K. Dashed lines represent the Redlich−Kister correlation between density and temperature for CO_2-loaded solutions.

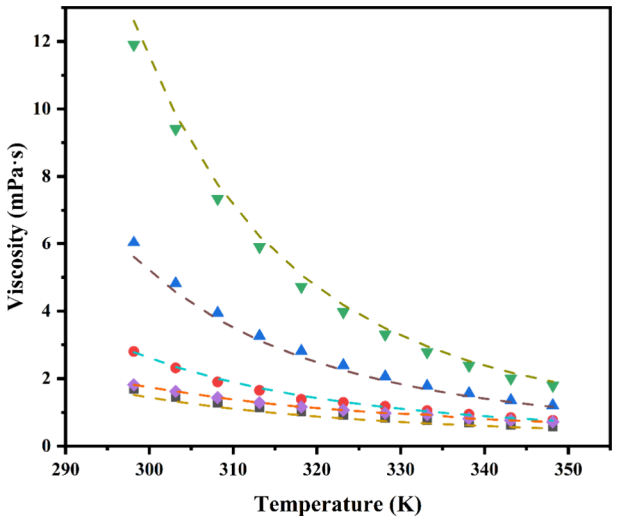

Figure 5. Viscosity of unloaded aqueous 1-MPZ solutions at various temperatures and concentrations (mass fraction): green triangles, 0.4; blue triangles, 0.3; circles, 0.2; squares, 0.1; diamonds, 1.0. The dashed lines in the graph represent viscosity results using the Grunberg and Nissan model.

that it contains and the molecular interactions between them.[46] From the results, it is found that the viscosity decreases with an increase in temperature. With an increase in concentration, the viscosity of aqueous 1-MPZ solutions increases. The viscosity results are presented in Figure 5. A stiff decrease in the viscosity of solutions with a higher concentration of 1-MPZ is observed in Figure 5. With the decrease in the concentration of 1-MPZ, the slope becomes moderate. The solvent having lower viscosity is more favorable for CO_2 absorption via the PCC method.

The experimental data of the binary viscosity of 1-MPZ + H_2O have been estimated using the model named the Grunberg and Nissan model.[40,41] The estimation of 1-MPZ + H_2O viscosity in unloaded solutions has been made using the expression shown in eq 11.

$$\ln \mu_m \text{ (mPa·s)} = \sum x_i \ln \mu_i + \sum \sum x_i x_j G_{ij} \quad (11)$$

where μ_i is the viscosity of the pure component i; x_i is the mole fraction of component i. G_{ij} is the temperature-dependent regressed coefficient given by eq 12.

$$G_{ij} = l + mT + nT^2 \quad (12)$$

In the present work, there is a binary system 1-MPZ + H_2O for which the above eq 11 can be expressed as the following eq 13.

$$\ln \mu_m = x_1 \ln \mu_1 + x_2 \ln \mu_2 + x_1 x_2 G_{12} \quad (13)$$

Table 8 shows the constants determined via the regression analysis of eq 12. Fifty-five data points were used to estimate

Table 8. Parameters of the Grunberg and Nissan Model in Equation 13, for the Viscosity of 1-MPZ (1) + H_2O (2)

parameter		1-MPZ + H_2O
G_{12}	l	267.3232
	m	−1.313680
	n	0.001702

Table 7. Viscosity of Unloaded Aqueous and Pure 1-MPZ Solutions at Atmospheric Pressure[a]

	viscosity η (mPa·s)				
T/K	w(1-MPZ) = 0.1	w(1-MPZ) = 0.2	w(1-MPZ) = 0.3	w(1-MPZ) = 0.4	w(1-MPZ) = 1.0
298.15	1.696	2.802	6.033	11.899	1.817
303.15	1.462	2.317	4.814	9.405	1.621
308.15	1.288	1.902	3.938	7.341	1.440
313.15	1.144	1.651	3.261	5.899	1.287
318.15	1.030	1.387	2.812	4.72	1.161
323.15	0.932	1.295	2.395	3.974	1.070
328.15	0.841	1.180	2.061	3.307	0.980
333.15	0.765	1.051	1.781	2.785	0.936
338.15	0.697	0.946	1.562	2.384	0.821
343.15	0.629	0.847	1.359	2.009	0.765
348.15	0.583	0.764	1.208	1.796	0.716

[a]The uncertainties are given in Table 15.

https://doi.org/10.1021/acs.jced.3c00651
J. Chem. Eng. Data 2024, 69, 904−914

the regression parameters. The AAD% within the experimental and associated model data is 5%.

Viscosity for CO_2-loaded aqueous 1-MPZ was measured in the same instrument, following the same procedure for temperature T = 298.15 to 328.15 K. Results are presented in Table 9. Figure 6 presents the viscosity results of CO_2-loaded 0.3w aqueous 1-MPZ. It is observed from Figure 6 that the viscosity of the CO_2-loaded solution first decreases when CO_2 is introduced into the amine solution. After that, the viscosity increases and stabilizes with the CO_2 loading. When gaseous CO_2 goes into the liquid, the fluidity of the liquid increases with the gas molecules, resulting in a decrease in viscosity. This phenomenon is also used in enhanced oil recovery by CO_2 flooding. In the secondary crude oil extraction process from oil fields, the oil can be extracted by injecting CO_2 into the oil rock. The CO_2 would gradually dissolve in the crude oil, resulting in a volume expansion and a decrease in the viscosity of the crude oil. Hence, crude oil can flow easily in porous rocks. The same behavior was observed in this CO_2-loaded aqueous solution of 1-MPZ. Interaction between CO_2 and the amine present in the aqueous solution results in carbamates and bicarbonate ions forming. The initial decrease in viscosity can be explained by the increase in the size of moieties due to the formation of anions, as the increase in size of the ion decreases viscosity.[47] As the concentration of CO_2 increases, the concentrations of carbamates and bicarbonate also increase in solution. These ions increase intermolecular interactions, resulting in an increase in viscosity with an increasing concentration of CO_2.[38]

Table 9. Viscosity of CO_2-Loaded Aqueous 1-MPZ Solutions at Atmospheric Pressure[a]

	loading α (mol CO_2/mol 1-MPZ)					
T/K	0	0.035	0.075	0.15	0.27	0.45
298.15	6.033	5.000	5.423	6.085	6.282	6.631
303.15	4.814	3.916	4.081	4.352	4.546	5.152
308.15	3.938	3.068	3.396	3.676	3.897	4.347
313.15	3.261	2.377	2.820	3.124	3.360	3.774
318.15	2.812	1.921	2.443	2.674	2.895	3.283
323.15	2.395	1.587	2.135	2.612	2.786	3.181
328.15	2.061	1.522	1.792	2.030	2.179	2.487

[a]The uncertainties are given in Table 15. w(1-methylpiperazine) = 0.3.

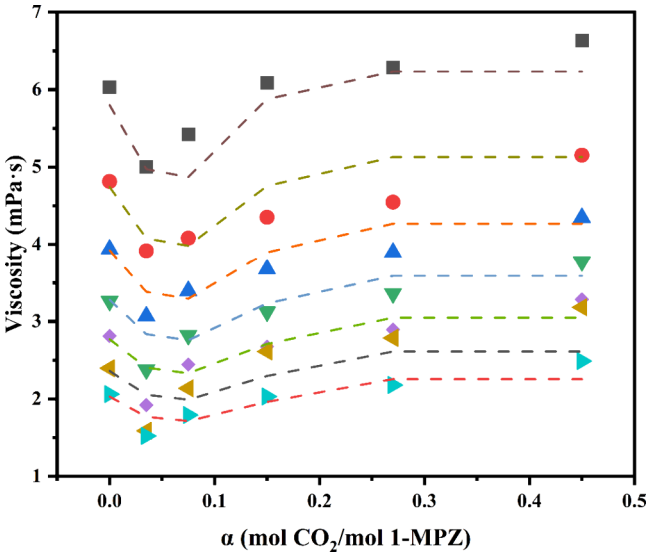

Figure 6. Viscosity of CO_2-loaded 0.3w aqueous 1-MPZ solutions at various temperatures: squares, 298.15 K; circles, 303.15 K; blue triangles, 308.15 K; green triangles, 313.15 K; diamonds, 318.15 K; yellow triangles, 323.15 K; cyan triangles, 328.15 K. Dashed lines represent results of modified Weiland's correlation.

The viscosity measured data for CO_2-loaded aqueous 0.3w 1-MPZ solutions have been correlated using Weiland's model.[48] In this model, the CO_2 loading has been replaced by the mole fraction of CO_2 in the liquid phase.[38] It is represented by eq 14.

$$\frac{\mu}{\mu_{H_2O}} = \exp\left[\frac{[(ax_1 + b)T + (cx_1 + d)][x_3(ex_1 + fT + g) + 10^3](x_1)}{T^2}\right] \quad (14)$$

where μ represents the experimental viscosity of the CO_2-loaded aqueous 1-MPZ solution, μ_{H_2O} is the viscosity of water, x_1 is the mole fraction of 1-MPZ, and x_3 is the mole fraction of CO_2.

The data fit accuracy (AAD%) with this model was determined to be 6.69%. The obtained parameters shown in eq 14 are reported in Table 10 using a total of 42 data points.

Table 10. Modified Weiland's Correlation Parameters for Loaded Viscosity (Equation 14)

parameters	value
a	−5320.960
b	373.1482
c	2,734,081
d	−191,062.0
e	-9.5×10^7
f	−292.2530
g	6,903,365

3.3. Surface Tension. The surface tension of 1-MPZ is performed in the temperature range of 303.15 to 348.15 K with an interval of 5 K. Table 11 represents the surface tension of 1-MPZ for different concentrations and temperatures. It is observed that when a small amount of 1-MPZ is added to water, it decreases the surface tension significantly. Pure 1-MPZ has the lowest surface tension value. So, with an increased concentration and temperature, the surface tension of aqueous 1-MPZ decreases. Experimental values and literature values of Rayer et al.[25] for pure 1-MPZ are compared and listed in Table S7.

A correlation for surface tension has been developed using a linear relation suggested by Venkat et al.,[49] which is a function of temperature for different mass fractions given by the expression shown in eq 15.

$$\gamma(\mathrm{mN{\cdot}m^{-1}}) = k_1 + k_2 T(K) \quad (15)$$

The parameters k_1 and k_2 of eq 15 are presented in Table 12 and are calculated through a linear regression analysis using 50 data points. The AAD% between the modeled surface tension data and experimental data is about 0.48%. Obtained results are compared with experimental results through a graphical representation in Figure 7.

The surface tension of the CO_2-loaded aqueous 1-MPZ is studied following the same method for temperatures ranging from 298.15 to 328.15 K. The results obtained are listed in

https://doi.org/10.1021/acs.jced.3c00651
J. Chem. Eng. Data 2024, 69, 904−914

Table 11. Surface Tension of Unloaded Aqueous and Pure 1-MPZ Solutions at Atmospheric Pressure[a]

	surface tension γ (mN/m)				
T/K	w(1-MPZ) = 0.1	w(1-MPZ) = 0.2	w(1-MPZ) = 0.3	w(1-MPZ) = 0.4	w(1-MPZ) = 1.0
303.15	52.42	50.42	49.82	45.44	30.01
308.15	52.31	49.92	49.05	44.34	29.19
313.15	51.65	49.35	48.46	43.76	28.56
318.15	51.03	48.99	47.91	43.15	27.74
323.15	50.35	48.39	47.28	42.73	27.31
328.15	49.38	47.98	46.55	42.14	26.21
333.15	48.59	47.56	45.94	41.53	25.18
338.15	47.54	46.93	44.95	40.83	24.47
343.15	47.07	46.24	43.89	40.15	23.36
348.15	46.32	45.63	42.82	38.95	21.90

[a]The uncertainties are given in Table 15.

Table 12. Regressed Parameters for the Surface Tension Data (H_2O + 1-MPZ) from Equation 15

mass fraction of 1-MPZ + H_2O	k_1	k_2
0.1 + 0.9	97.1612	−0.14585
0.2 + 0.8	81.9261	−0.10375
0.3 + 0.7	95.2970	−0.14934
0.4 + 0.6	84.8287	−0.13060
1 + 0	82.8019	−0.17323

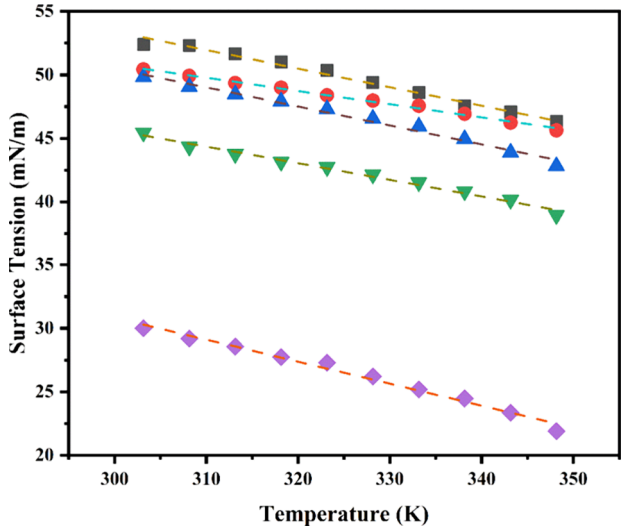

Figure 7. Surface tension of unloaded aqueous 1-MPZ solutions at various temperatures and concentrations (mass fraction): green triangles, 0.4; blue triangles, 0.3; circles, 0.2; squares, 0.1; diamonds, 1.0. Modeled surface tension results from eq 15 are represented by using dashed lines.

Table 13, and the surface tension of loaded and unloaded 0.3w 1-MPZ is plotted in Figure 8. It is observed that initially, when CO_2 interacts with 1-MPZ, the surface tension of the solvent increases. However, with the increase in the loading of CO_2, surface tension starts decreasing. The temperature dependency of the CO_2-loaded solvent was found to be irregular at slightly higher temperatures. A crossover is observed in loaded surface tension results in between loadings. This could be due to the increase in surface tension with an increase in temperature for higher-temperature CO_2-loaded solutions. Further investigation is required to understand this behavior of the solvent.

Surface tension data for the loaded solutions presented in this work are correlated with a polynomial function of CO_2 loading α and temperature T, suggested by Jayarathna et al.[50] The working equation has the format of eq 16.

$$\gamma\ (\mathrm{mN\cdot m^{-1}}) = p_1 + p_2\alpha + p_3T + p_4\alpha^2 + p_5\alpha T + p_6T^2 + p_7\alpha^3 + p_8\alpha^2T + p_9T^2\alpha + p_{10}\alpha^4 + p_{11}\alpha^3T + p_{12}\alpha^2T^2 \quad (16)$$

Table 13. Surface Tension of CO_2-Loaded Aqueous 1-MPZ Solutions at Atmospheric Pressure[a]

	loading α (mol CO_2/mol 1-MPZ)					
T/K	0	0.035	0.075	0.15	0.27	0.45
303.15	49.82	52.50	45.91	42.25	37.36	34.20
308.15	49.05	50.49	44.72	40.19	37.04	35.47
313.15	48.46	49.67	43.92	39.85	37.30	35.53
318.15	47.91	48.92	43.12	39.83	37.56	35.78
323.15	47.28	48.01	42.97	39.96	38.17	35.64
328.15	46.55	46.80	42.91	39.86	38.79	34.95

[a]The uncertainties are given in Table 15. w(1-methylpiperazine) = 0.3.

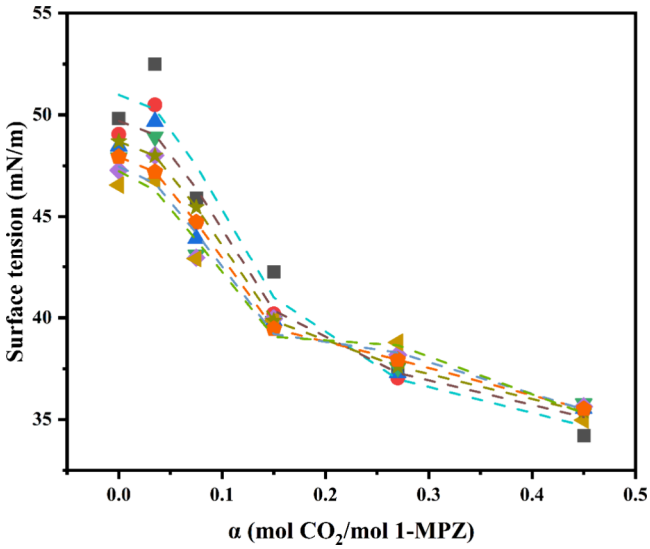

Figure 8. Surface tension of CO_2-loaded 0.3w aqueous 1-MPZ at various temperatures: squares, 303.15 K; circles, 308.15 K; blue triangles, 313.15 K; green triangles, 318.15 K; diamonds, 323.15 K; yellow triangles, 328.15 K. Dashed lines represent modeled surface tension results using eq 16.

https://doi.org/10.1021/acs.jced.3c00651
J. Chem. Eng. Data 2024, 69, 904−914

where $p_i's$ are the regressed coefficients of eq 16. The values of the coefficients are listed in Table 14. Using 36 data points, the following results of parameters are calculated. The modeled surface tension data show 1.69 AAD% with experimental data.

Table 14. Estimated Parameters of Surface Tension of the CO_2-Loaded 0.3*w* Aqueous 1-MPZ Solution (Equation 16)

parameters	value	parameters	value
p_1	623.259	p_7	9832.63
p_2	−1649.55	p_8	4.57105
p_3	−3.49317	p_9	−0.01849
p_4	−4036.97	p_{10}	−5693.15
p_5	11.0938	p_{11}	−16.4905
p_6	0.00529	p_{12}	5.00622

The surface tension result of pure 1-MPZ is compared with literature values of pure MDEA and pure MEA and presented in Figure S3 in the Supporting Information. Vázquez et al.[32] reported surface tension data for pure MEA that is considered for comparison. Pure MDEA results are compared with 1-MPZ reported by Alvarez et al.[51] From Figure S3, it is observed that 1-MPZ has lower values of surface tension than pure MEA and MDEA.

4. UNCERTAINTY IN EXPERIMENTAL RESULTS

Uncertainties in the results depend on the standard uncertainties of individual components (Table 15). Combining

Table 15. Uncertainties in Experiments of Density, Viscosity, and Surface Tension Measurements[a]

	density measurement	viscosity measurement	surface tension measurement
$u(T)$	0.03 K	0.1 K	0.3 K
$u(w)$	1×10^{-6}	1×10^{-6}	1×10^{-6}
instrument accuracy	0.05 kg·m^{-3}	0.05 mPa·s	0.2 mN/m
$u_r(\alpha)$	0.03 mol CO_2/mol 1-MPZ	0.03 mol CO_2/mol 1-MPZ	0.03 mol CO_2/mol 1-MPZ
U_c of unloaded 1-MPZ solutions	0.559 kg·m^{-3}	0.410 mPa·s	0.731 mN/m
U_c of CO_2-loaded 1-MPZ solutions	1.521 kg·m^{-3}	0.869 mPa·s	1.673 mN/m

[a] u is the standard uncertainty, u_r is the relative standard uncertainty, and U_c is the expanded uncertainty at the 0.95 level of confidence.

all of the legal uncertainties of all of the affecting factors gives an actual uncertainty of outcomes. Factors affecting density measurement are the temperature accuracy of the instrument, error in the weighing balance, and instrumental error of the density meter DMA 4500M. The uncertainty of a sample impurity is incorporated in expanded uncertainty as explained by Chirico et al.[52] The temperature accuracy of the instrument is 0.03 K. The instrument accuracy of DMA 4500M is 0.05 kg·m^{-3}. The accuracy of the weight of 1-MPZ is 0.002 g. All of these individual uncertainties are combined using a root sum of squares (RSS) formula to get the expanded uncertainty of unloaded density measurement. Similarly, for loaded 1-MPZ solutions, the relative uncertainty of CO_2 loading, which is 0.03 mol CO_2/mol 1-MPZ, is also considered. The level of confidence is 0.95 ($K = 2$).

Similarly, standard errors of individual sources are incorporated using the RSS equation for surface tension and viscosity measurement. The accuracy of the Cannon Fenske viscometer is 0.05 mPa·s, while for a surface tensiometer, the accuracy is 0.2 mN/m.

5. CONCLUSIONS

Physicochemical properties are essential to understanding solvent compatibility for CO_2 capture using the PCC process, where regenerative chemical absorption of CO_2 is adapted and the solvent plays a crucial role. In this work to formulate a CO_2 capture solvent, the density, viscosity, and surface tension of 1-MPZ have been studied for the pure solution and its aqueous solutions of different concentrations for temperatures ranging from 298.15 to 348.15 K. The results were found to be highly dependent on the concentration of the solvent as well as temperature. Volumetric properties are crucial to understanding the interaction between the solvent and the solute. The excess molar volume is calculated from density values. CO_2-loaded properties of the 0.3*w* 1-MPZ solution have been studied. The concentration of CO_2 was gradually increased to 0.45 mol CO_2/mol 1-MPZ. Density, viscosity, and surface tension have been studied for this CO_2-loaded solution for temperatures from 298.15 to 328.15 K. The density increases with an increase in the concentration of CO_2. The viscosity of CO_2-loaded 1-MPZ first decreases at the lowest concentration but gradually increases and stabilizes with an increasing concentration of CO_2.

In surface tension, when CO_2 is introduced in solution, values increase drastically, but with an increasing concentration of CO_2, they tend to decrease. All of the CO_2-loaded and unloaded experimental results have been correlated through modeling using various approaches. All the experimental results are in good agreement with the modeling results. Modeling results of unloaded solutions have lower deviations from experimental results when compared to those of CO_2-loaded solutions. This may be due to the increased uncertainty in experimental results due to the three-component system (1-MPZ + H_2O + CO_2). Lower viscosity and surface tension values make aqueous 1-MPZ a favorable solvent for PCC technology. These new data and model results of (1-MPZ + H_2O + CO_2) will be essential for process design and to estimate diffusivities, which is required for rate-kinetic model development of the CO_2 reaction in those solvents and also to perform various fluid dynamics calculations in the PCC process.

■ ASSOCIATED CONTENT

Supporting Information

The Supporting Information is available free of charge at https://pubs.acs.org/doi/10.1021/acs.jced.3c00651.

Sample calculation of CO_2 loading; validation of the density difference method; CO_2 loading comparison; density, viscosity, and surface tension of unloaded 0.3 weight fraction MEA; density, viscosity, and surface tension of unloaded pure 1-MPZ; parity plot of the CO_2 loading; excess molar volume of unloaded aqueous 1-MPZ solutions; comparison of surface tension results (PDF)

■ AUTHOR INFORMATION

Corresponding Authors

Rajib Bandyopadhyay − *Department of Chemistry, Pandit Deendayal Energy University, Gandhinagar 382426, India;*

https://doi.org/10.1021/acs.jced.3c00651
J. Chem. Eng. Data 2024, 69, 904−914

orcid.org/0000-0003-0276-6678;
Email: Rajib.Bandyopadhyay@sot.pdpu.ac.in
Sukanta Kumar Dash − *Department of Chemical Engineering, Pandit Deendayal Energy University, Gandhinagar 382426, India*; orcid.org/0000-0003-2325-1294;
Email: sk.dash@sot.pdpu.ac.in, sukantakdash@gmail.com

Authors

Vaibhav Vamja − *Department of Chemistry, Pandit Deendayal Energy University, Gandhinagar 382426, India*
Chetna Shukla − *Department of Mathematics, Pandit Deendayal Energy University, Gandhinagar 382426, India*

Complete contact information is available at: https://pubs.acs.org/10.1021/acs.jced.3c00651

Author Contributions

V.V. performed formal analysis, investigation, methodologies, original draft preparation, and review and editing of the manuscript; C.S. performed modeling and writing of the draft. R.B. performed supervision and conceptualization. S.K.D. performed supervision, conceptualization, funding and resources acquisition, data curation, and project administration.

Notes

The authors declare no competing financial interest.

■ ACKNOWLEDGMENTS

This work was supported by the Department of Biotechnology, Ministry of Science and Technology, New Delhi, Govt. of India: No. BT/PR31120/PBD/26/755/2019, dated 13th February, 2020. The authors would like to express their sincere gratitude to SHODH fellowship (ref no. 2021015812) for financial support.

■ REFERENCES

(1) Shukla, C.; Mishra, P.; Dash, S. K. A review of process intensified CO_2 capture in RPB for sustainability and contribution to industrial net zero. *Front. Energy Res.* **2023**, *11*, No. 1135188.
(2) Lee, S.; Song, H.-J.; Maken, S.; Park, J.-W. Kinetics of CO_2 absorption in aqueous sodium glycinate solutions. *Industrial & engineering chemistry research* **2007**, *46* (5), 1578−1583.
(3) Ramezani, R.; Bernhardsen, I. M.; Di Felice, R.; Knuutila, H. K. Physical properties and reaction kinetics of CO2 absorption into unloaded and CO_2 loaded viscous monoethanolamine (MEA) solution. *J. Mol. Liq.* **2021**, *329*, No. 115569.
(4) Lee, S.; Maken, S.; Park, J.-W.; Song, H.-J.; Park, J. J.; Shim, J.-G.; Kim, J.-H.; Eum, H.-M. A study on the carbon dioxide recovery from 2 ton-CO_2/day pilot plant at LNG based power plant. *Fuel* **2008**, *87* (8−9), 1734−1739.
(5) Dash, S. K.; Bandyopadhyay, S. S. Studies on the effect of addition of piperazine and sulfolane into aqueous solution of N-methyldiethanolamine for CO_2 capture and VLE modelling using eNRTL equation. *International Journal of Greenhouse Gas Control* **2016**, *44*, 227−237.
(6) Dash, S. K.; Samanta, A. N.; Bandyopadhyay, S. S. (Vapour+ liquid) equilibria (VLE) of CO_2 in aqueous solutions of 2-amino-2-methyl-1-propanol: New data and modelling using eNRTL-equation. *J. Chem. Thermodyn.* **2011**, *43* (8), 1278−1285.
(7) Song, H.-J.; Lee, S.; Maken, S.; Ahn, S.-W.; Park, J.-W.; Min, B.; Koh, W. Environmental and economic assessment of the chemical absorption process in Korea using the LEAP model. *Energy Policy* **2007**, *35* (10), 5109−5116.
(8) Darji, M.; Manhas, A.; Dash, S. K.; Mukherjee, K. Dissociation Constants of Amine Solvents Used in CO_2 Capture: Titrimetric Estimation and Density Functional Theory Calculation. *Ind. Eng. Chem. Res.* **2023**, 7868.
(9) Rayer, A. V.; Sumon, K. Z.; Henni, A.; Tontiwachwuthikul, P. Kinetics of the reaction of carbon dioxide (CO_2) with cyclic amines using the stopped-flow technique. *Energy Procedia* **2011**, *4*, 140−147.
(10) Gordesli, F. P.; Alper, E. The kinetics of carbon dioxide capture by solutions of piperazine and N-methyl piperazine. *International Journal of Global Warming* **2011**, *3* (1−2), 67−76.
(11) Dash, S. K.; Samanta, A. N.; Bandyopadhyay, S. S. Experimental and theoretical investigation of solubility of carbon dioxide in concentrated aqueous solution of 2-amino-2-methyl-1-propanol and piperazine. *J. Chem. Thermodyn.* **2012**, *51*, 120−125.
(12) Dey, A.; Dash, S. K.; Balchandani, S. C.; Mandal, B. Investigation on the inclusion of 1-(2-aminoethyl) piperazine as a promoter on the equilibrium CO_2 solubility of aqueous 2-amino-2-methyl-1-propanol. *J. Mol. Liq.* **2019**, *289*, No. 111036.
(13) Chen, X.; Rochelle, G. T. Aqueous piperazine derivatives for CO_2 capture: Accurate screening by a wetted wall column. *Chem. Eng. Res. Des.* **2011**, *89* (9), 1693−1710.
(14) Li, H.; Le Moullec, Y.; Lu, J.; Chen, J.; Marcos, J. C. V.; Chen, G. Solubility and energy analysis for CO_2 absorption in piperazine derivatives and their mixtures. *Int. J. Greenhouse Gas Control* **2014**, *31*, 25−32.
(15) Song, H.-J.; Lee, S.; Maken, S.; Park, J.-J.; Park, J.-W. Solubilities of carbon dioxide in aqueous solutions of sodium glycinate. *Fluid Phase Equilib.* **2006**, *246* (1−2), 1−5.
(16) Lee, S.; Song, H.-J.; Maken, S.; Shin, H.-C.; Song, H.-C.; Park, J.-W. Physical solubility and diffusivity of N_2O and CO_2 in aqueous sodium glycinate solutions. *Journal of Chemical & Engineering Data* **2006**, *51* (2), 504−509.
(17) Li, H.; Le Moullec, Y.; Lu, J.; Chen, J.; Marcos, J. C. V.; Chen, G.; Chopin, F. CO_2 solubility measurement and thermodynamic modeling for 1-methylpiperazine/water/CO_2. *Fluid Phase Equilib.* **2015**, *394*, 118−128.
(18) Rayer, A. V.; Armugam, Y.; Henni, A.; Tontiwachwuthikul, P. High-pressure solubility of carbon dioxide (CO_2) in aqueous 1-methyl piperazine solution. *Journal of Chemical & Engineering Data* **2014**, *59* (11), 3610−3623.
(19) Kumari, K.; Maken, S. Topological investigation of intermolecular interactions in di-isopropylamine (DIPA)+ isomeric butanol mixtures: Volumetric and acoustic properties. *J. Mol. Liq.* **2021**, *325*, No. 115170.
(20) Lee, S.; Song, H.-J.; Maken, S.; Yoo, S.-K.; Park, J.-W.; Kim, S.; Shim, J. G.; Jang, K.-R. Simulation of CO_2 removal with aqueous sodium glycinate solutions in a pilot plant. *Korean Journal of Chemical Engineering* **2008**, *25*, 1−6.
(21) Idris, Z.; Chen, J.; Eimer, D. A. Densities of unloaded and CO_2-loaded 3-dimethylamino-1-propanol at temperatures (293.15 to 343.15) K. *J. Chem. Thermodyn.* **2016**, *97*, 282−289.
(22) Lee, S.; Choi, S.-I.; Maken, S.; Song, H.-J.; Shin, H.-C.; Park, J.-W.; Jang, K.-R.; Kim, J.-H. Physical properties of aqueous sodium glycinate solution as an absorbent for carbon dioxide removal. *Journal of Chemical & Engineering Data* **2005**, *50* (5), 1773−1776.
(23) Kumari, M.; Vega, F.; Fernández, L. M. G.; Shadangi, K. P.; Kumar, N. Liquid Amine functional, aqueous blends and the CO_2 absorption capacity: molecular structure, size, interaction parameter and mechanistic aspects. *J. Mol. Liq.* **2023**, *384*, No. 122288.
(24) Idris, Z.; Han, J.; Jayarathna, S.; Eimer, D. A. Surface tension of alkanolamine solutions: an experimentally based review. *Energy Procedia* **2017**, *114*, 1828−1833.
(25) Rayer, A. V.; Sumon, K. Z.; Henni, A.; Tontiwachwuthikul, P. Physicochemical properties of {1-methyl piperazine (1)+ water (2)} system at T = (298.15 to 343.15) K and atmospheric pressure. *J. Chem. Thermodyn.* **2011**, *43* (12), 1897−1905.
(26) Chen, S.; Lei, Q.; Fang, W. Density and Refractive Index at 298.15 K and Vapor− Liquid Equilibria at 101.3 kPa for Four Binary Systems of Methanol, n-Propanol, n-Butanol, or Isobutanol with N-Methylpiperazine. *Journal of Chemical & Engineering Data* **2002**, *47* (4), 811−815.
(27) Chen, S.-d.; Lei, Q.-f.; Fang, W.-j. Viscosities and densities for binary mixtures of N-methylpiperazine with methanol, ethanol, n-

propanol, iso-propanol, n-butanol and iso-butanol at 293.15, 298.15 and 303.15 K. *Fluid phase equilibria* **2005**, *234* (1−2), 22−33.
(28) Yang, X.; Xing, Y.; Li, D.; Guo, Y.; Fang, W. Volumetric and viscous properties at several temperatures for binary mixtures of n-methylpiperazine with methylcyclohexane or n-heptane. *Journal of Chemical & Engineering Data* **2010**, *55* (8), 2914−2916.
(29) Dash, S. K.; Samanta, A. N.; Bandyopadhyay, S. S. Simulation and parametric study of post combustion CO_2 capture process using (AMP+ PZ) blended solvent. *International Journal of Greenhouse Gas Control* **2014**, *21*, 130−139.
(30) Hartono, A.; Mba, E. O.; Svendsen, H. F. Physical properties of partially CO_2 loaded aqueous monoethanolamine (MEA). *Journal of Chemical & Engineering Data* **2014**, *59* (6), 1808−1816.
(31) Amundsen, T. G.; Øi, L. E.; Eimer, D. A. Density and viscosity of monoethanolamine+ water+ carbon dioxide from (25 to 80) C. *Journal of Chemical & Engineering Data* **2009**, *54* (11), 3096−3100.
(32) Vázquez, G.; Alvarez, E.; Navaza, J. M.; Rendo, R.; Romero, E. Surface tension of binary mixtures of water+ monoethanolamine and water+ 2-amino-2-methyl-1-propanol and tertiary mixtures of these amines with water from 25 to 50 C. *Journal of Chemical & Engineering Data* **1997**, *42* (1), 57−59.
(33) Freeman, S. A.; Dugas, R.; Van Wagener, D. H.; Nguyen, T.; Rochelle, G. T. Carbon dioxide capture with concentrated, aqueous piperazine. *International Journal of Greenhouse Gas Control* **2010**, *4* (2), 119−124.
(34) Han, J.; Jin, J.; Eimer, D. A.; Melaaen, M. C. Density of Water (1)+ Monoethanolamine (2)+ CO_2 (3) from (298.15 to 413.15) K and Surface Tension of Water (1)+ Monoethanolamine (2) from (303.15 to 333.15) K. *Journal of Chemical & Engineering Data* **2012**, *57* (4), 1095−1103.
(35) Ma'mun, S.; Jakobsen, J. P.; Svendsen, H. F.; Juliussen, O. Experimental and modeling study of the solubility of carbon dioxide in aqueous 30 mass% 2-((2-aminoethyl) amino) ethanol solution. *Industrial & engineering chemistry research* **2006**, *45* (8), 2505−2512.
(36) Wagner, M.; von Harbou, I.; Kim, J.; Ermatchkova, I.; Maurer, G.; Hasse, H. Solubility of carbon dioxide in aqueous solutions of monoethanolamine in the low and high gas loading regions. *Journal of Chemical & Engineering Data* **2013**, *58* (4), 883−895.
(37) Xie, H.-B.; Zhou, Y.; Zhang, Y.; Johnson, J. K. Reaction mechanism of monoethanolamine with CO_2 in aqueous solution from molecular modeling. *J. Phys. Chem. A* **2010**, *114* (43), 11844−11852.
(38) Karunarathne, S. S.; Eimer, D. A.; Øi, L. E. Density, viscosity and free energy of activation for viscous flow of CO_2 loaded 2-amino-2-methyl-1-propanol (AMP), monoethanol amine (MEA) and H_2O mixtures. *J. Mol. Liq.* **2020**, *311*, No. 113286.
(39) Luo, X.; Su, L.; Gao, H.; Wu, X.; Idem, R. O.; Tontiwachwuthikul, P.; Liang, Z. Density, viscosity, and N_2O solubility of aqueous 2-(methylamino) ethanol solution. *Journal of Chemical & Engineering Data* **2017**, *62* (1), 129−140.
(40) Paul, S.; Mandal, B. Density and Viscosity of Aqueous Solutions of (N-Methyldiethanolamine+ Piperazine) and (2-Amino-2-methyl-1-propanol+ Piperazine) from (288 to 333) K. *Journal of Chemical & Engineering Data* **2006**, *51* (5), 1808−1810.
(41) Dey, A.; Dash, S. K.; Mandal, B. Equilibrium CO_2 solubility and thermophysical properties of aqueous blends of 1-(2-aminoethyl) piperazine and N-methyldiethanolamine. *Fluid Phase Equilib.* **2018**, *463*, 91−105.
(42) Kumari, K.; Maken, S. Volumetric, acoustic, transport and FTIR studies of binary di-butylamine+ isomeric butanol mixtures as potential CO = 2 absorbents. *J. Mol. Liq.* **2021**, *326*, No. 115253.
(43) Verma, S.; Bhagat, P.; Gahlyan, S.; Rani, M.; Kumar, N.; Malik, R. K.; Lee, Y.; Maken, S. Thermophysical properties of N-isopropyl-2-propanamine+ alkanol (C1-C3) mixtures as absorbents for carbon dioxide capture. *Korean J. Chem. Eng.* **2023**, *40*, 1−10.
(44) Hawrylak, B.; Burke, S. E.; Palepu, R. Partial molar and excess volumes and adiabatic compressibilities of binary mixtures of ethanolamines with water. *Journal of solution chemistry* **2000**, *29*, 575−594.
(45) Bhagat, P.; Maken, S. Modeling of transport and volumetric properties of tributylamine based absorbents for CO_2 capture. *J. Mol. Liq.* **2021**, *326*, No. 115240.
(46) Verma, S.; Bhagat, P.; Gahlyan, S.; Rani, M.; Kumar, N.; Malik, R. K.; Lee, Y.; Maken, S. Thermophysical properties of 2-amino-2-methylpropan-1-ol+ alkanol mixtures: Investigation of molecular interactions by insight of FT-IR spectroscopy. *J. Mol. Liq.* **2023**, *382*, No. 121967.
(47) Silva, W.; Zanatta, M.; Ferreira, A. S.; Corvo, M. C.; Cabrita, E. J. Revisiting ionic liquid structure-property relationship: A critical analysis. *International journal of molecular sciences* **2020**, *21* (20), 7745.
(48) Weiland, R. H.; Dingman, J. C.; Cronin, D. B.; Browning, G. J. Density and viscosity of some partially carbonated aqueous alkanolamine solutions and their blends. *Journal of Chemical & Engineering Data* **1998**, *43* (3), 378−382.
(49) Venkat, A.; Kumar, G.; Kundu, M. Density and Surface Tension of Aqueous Solutions of (2-(Methylamino)-ethanol+ 2-Amino-2-methyl-1-propanol) and (2-(Methylamino)-ethanol+ N-Methyl-diethanolamine) from (298.15 to 323.15) K. *Journal of Chemical & Engineering Data* **2010**, *55* (11), 4580−4585.
(50) Jayarathna, S. A.; Weerasooriya, A.; Dayarathna, S.; Eimer, D. A.; Melaaen, M. C. Densities and surface tensions of CO_2 loaded aqueous monoethanolamine solutions with r = (0.2 to 0.7) at T = (303.15 to 333.15) K. *Journal of Chemical & Engineering Data* **2013**, *58* (4), 986−992.
(51) Alvarez, E.; Rendo, R.; Sanjurjo, B.; Sanchez-Vilas, M.; Navaza, J. M. Surface tension of binary mixtures of water+ N-methyldiethanolamine and ternary mixtures of this amine and water with monoethanolamine, diethanolamine, and 2-amino-2-methyl-1-propanol from 25 to 50 C. *Journal of Chemical & Engineering Data* **1998**, *43* (6), 1027−1029.
(52) Chirico, R. D.; Frenkel, M.; Magee, J. W.; Diky, V.; Muzny, C. D.; Kazakov, A. F.; Kroenlein, K.; Abdulagatov, I.; Hardin, G. R.; Acree, W. E. Jr.; Brenneke, J. F.; Brown, P. L.; Cummings, P. T.; de Loos, T. W.; Friend, D. G.; Goodwin, A. R. H.; Hansen, L. D.; Haynes, W. M.; Koga, N.; Mandelis, A.; Marsh, K. N.; Mathias, P. M.; McCabe, C.; O'Connell, J. P.; Pádua, A.; Rives, V.; Schick, C.; Trusler, J. P. M.; Vyazovkin, S.; Weir, R. D.; Wu, J. Improvement of quality in publication of experimental thermophysical property data: Challenges, assessment tools, global implementation, and online support. *J. Chem. Eng. Data* **2013**, *58* (10), 2699−2716.

https://doi.org/10.1021/acs.jced.3c00651
J. Chem. Eng. Data 2024, 69, 904−914